

## Divacancy-iron complexes in silicon

C. K. Tang,<sup>1,a)</sup> L. Vines,<sup>1</sup> V. P. Markevich,<sup>2</sup> B. G. Svensson,<sup>1</sup> and E. V. Monakhov<sup>1</sup>

<sup>1</sup>Physics Department/Center for Materials Science and Nanotechnology, University of Oslo, P.O. Box 1048 Blindern, N-0316 Oslo, Norway

<sup>2</sup>School of Electrical and Electronic Engineering, Photon Science Institute, University of Manchester, Manchester M13 9PL, Lancs, England

(Received 25 October 2012; accepted 26 December 2012; published online 22 January 2013)

Iron and irradiation-induced defects have been investigated in p-type float-zone silicon after MeV electron-irradiation using deep level transient spectroscopy. Isochronal annealing (30 min) was performed up to 250 °C, and three distinctive energy levels are observed in the Fe-contaminated samples with positions of 0.25, 0.29, and 0.34 eV above the valence band edge, respectively. The two latter ones are found to accompany the change in concentration of the divacancy center ( $V_2$ ) during the isochronal annealing which strongly indicates an interaction between Fe and  $V_2$ . Furthermore, the properties of the defects support recent theoretical predictions of  $FeV_2$  and  $VFeV$  (Estreicher *et al.*, Phys. Rev. B **77**, 125214 (2008)). © 2013 American Institute of Physics. [<http://dx.doi.org/10.1063/1.4788695>]

### I. INTRODUCTION

Iron is well-known for its detrimental effects on the performance of silicon solar cells and integrated circuits.<sup>1</sup> Solar cells based on p-type silicon can be significantly improved by gettering during a phosphorus in-diffusion step which accumulates Fe close to the surface and reduces its concentration in the bulk. Although this process is commonly employed, the underlying mechanism of the gettering of Fe is not fully understood. Furthermore, solar cells receiving the phosphorus gettering may still exhibit light-induced degradation with degradation characteristics of Fe contamination.<sup>2</sup>

To further improve the gettering efficiency of Fe, it is important to understand the underlying mechanism and the defects formed during the gettering. Recently, it was shown that the major contribution of Fe gettering did not occur by the formation of a phosphorus-iron complex, where intentionally introduced Fe was gettering with a similar concentration versus depth profile regardless of the phosphorus depth profile.<sup>3</sup> In Ref. 3, a mechanism involving oxygen and vacancies, injected during the phosphorus in-diffusion, was proposed.

Indeed, a reaction between the vacancy-oxygen complex and Fe has been reported in n-type silicon by You *et al.*,<sup>4</sup> using deep level transient spectroscopy (DLTS), and the defect was shown to be stable up to 300 °C. The disappearance of the DLTS signal was suggested to be caused by the formation of a more stable complex, presumably substitutional Fe and interstitial oxygen. Furthermore, although not discussed in Ref. 4, the divacancy center ( $V_2$ ) decreases in concentration after annealing at 80 °C for 2.5 h, suggesting a reaction between  $V_2$  and Fe. This is also addressed by Komarov,<sup>5</sup> who investigated reactions between irradiation-induced defects with residual impurities in n-type silicon. Komarov observed the appearance of a hole trap at 0.184 eV above the valence band edge ( $E_V$ ) after annealing at 150 °C

which remained stable at 400 °C. Tentatively, this defect was assigned to  $FeV_2$ , with the basic argument that Fe was present in the samples.

Theoretical results have recently been reported on the interaction between irradiation-induced defects and Fe.<sup>6</sup> The calculations predict two stable complexes between  $V_2$  and Fe. The one with the lowest total energy is labelled as  $VFeV$ , where the Fe is situated half way between two vacancies. This configuration has a single acceptor level at  $E_V + 0.38$  eV ( $E_C - 0.73$  eV, where  $E_C$  is the conduction band edge) and a double acceptor level at  $E_C - 0.55$  eV. The other configuration is  $FeV_2$  which has one donor level at  $E_V + 0.25$  eV and one acceptor level at  $E_V + 0.36$  eV ( $E_C - 0.75$  eV).

Recently, we have investigated the interaction between Fe and proton-irradiation-induced defects in p-type silicon using DLTS after isochronal annealing.<sup>7</sup> Several Fe-related defects were observed, and one appeared after 150 °C with an energy level position of  $E_V + 0.28$  eV, labelled as H(0.28). Based on the evolution of the concentrations of H(0.28) and  $V_2$ , H(0.28) was tentatively assigned as a divacancy-Fe complex, although, the involvement of hydrogen (arising from proton-implantation) could not be ruled out.

In this study, Fe-contaminated and Fe-lean float-zone (Fz) p-type silicon samples have been irradiated by electrons and investigated for possible reactions of Fe with irradiation-induced defects. Several deep level defects are observed exclusively in the Fe-contaminated samples after annealing above 125 °C. Based on the evolution of the different defect concentrations as a function of annealing temperatures, there are strong indications that two of these defect levels originate from complexes of Fe and  $V_2$ .

### II. EXPERIMENT

Samples were cut from Fz boron-doped silicon with doping concentration of  $2 \times 10^{14} \text{ cm}^{-3}$  (resistivity of around 70  $\Omega \text{ cm}$ ), as confirmed by capacitance-voltage (CV) measurements. Dry oxidation was performed at 1000 °C for 8 h after a

<sup>a)</sup>Electronic mail: c.k.tang@smn.uio.no.

HF-dip, and circular holes of 2 mm in diameter were opened at the frontside using photolithography for the preparation of a pn-junction. Phosphorus was implanted at the frontside with an energy and fluence of 36 keV and  $1 \times 10^{14} \text{ cm}^{-2}$ , respectively. Thereafter, Fe was implanted at the rear side with energy and fluence of 700 keV and  $1 \times 10^{14} \text{ cm}^{-2}$ , respectively. After the implantation, the samples were heat treated at 875 °C for 1 h to activate the  $n^+$ -layer and to diffuse Fe to the frontside of the 500  $\mu\text{m}$  thick sample.<sup>8</sup>

Aluminium contacts of 1 mm in diameter were deposited onto the  $n^+$ -layer of the pn-junction, and Ohmic contacts were formed at the rear side by applying silver-paste. The samples were electrically characterized using CV-measurement and DLTS. For DLTS, six rate-windows were used ranging from  $(20 \text{ ms})^{-1}$  to  $(640 \text{ ms})^{-1}$  and the signals were typically extracted by the GS4 weighting function.<sup>9</sup> The reverse and pulse bias voltages were 4.5 and  $-4.5 \text{ V}$ , respectively.

After initial DLTS measurements, which confirmed that only the Fe-contaminated samples (and not the control ones) contained the Fe-B pair and/or interstitial Fe ( $\text{Fe}_i$ ) while other centers were below the detection limit, electron-irradiation was performed with an energy of 4 MeV and a fluence of  $2 \times 10^{14} \text{ cm}^{-2}$ . The reference samples, which had Al Schottky barrier contacts and were not phosphorus-implanted or intentionally contaminated with Fe, received the same electron-fluence. The electron-irradiated samples were stored for three weeks at room temperature before commencing characterization and isochronal annealing (30 min) from 125 to 250 °C with an interval of 25 °C.

### III. RESULTS AND DISCUSSION

Figure 1 shows the DLTS spectra of Fe-contaminated (Fig. 1(a)) and reference (Fig. 1(b)) samples in the as-implanted state and after annealing at 150, 200, and 250 °C. The ordinate in the temperature interval of 90 to 160 K has been enhanced by a factor 8 for clarity. Focusing on the as-implanted samples, prominent irradiation-induced defects can be observed both in the reference and the Fe-contaminated samples, such as the  $\text{V}_2$  (Refs. 10–12) and the interstitial carbon-oxygen pair ( $\text{C}_i\text{O}_i$ )<sup>11,13</sup> with the respective energy level positions of 0.18 eV and 0.35 eV above  $E_V$ . A small amount of interstitial carbon ( $\text{C}_i$ )<sup>13</sup> can also be observed at 139 K ( $\sim E_V + 0.30 \text{ eV}$ ), but it becomes negligible after annealing above room temperature.

In the Fe-contaminated samples (Fig. 1(a)), the Fe-B pair is observed at 47 K ( $\sim E_V + 0.10 \text{ eV}$ ) and with a concentration of  $1.7 \times 10^{13} \text{ cm}^{-3}$ . Fe-B can dissociate into  $\text{Fe}_i$  in a reversible reaction by heat treatment, illumination, or by minority carrier injection.<sup>8,14</sup>  $\text{Fe}_i$  occurs at  $E_V + 0.40 \text{ eV}$  and can be readily observed in Fig. 1 at 218 K after annealing at 150 °C. It should be mentioned that the sum of the concentration of the Fe-B pair and the  $\text{Fe}_i$  decreases by subsequent annealing.  $\text{Fe}_i$  is highly mobile and the decrease may be explained by migration to the surface, or reactions with other defects such as the irradiation-induced ones. Here, it should be pointed out that the Fe-contaminated samples, in contrast to the reference ones, have an  $n^+$ -surface layer formed by phosphorus implantation (and subsequent annealing). The

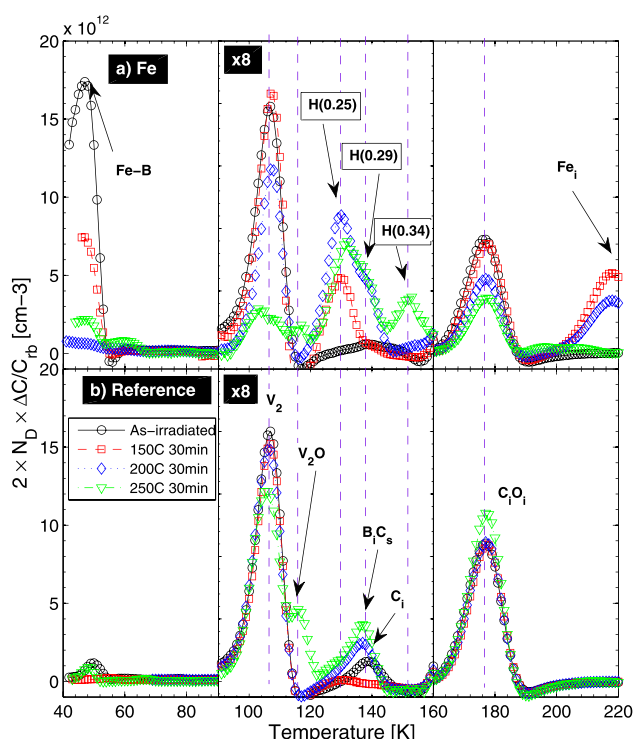


FIG. 1. Spectra of DLTS measurements, with GS4 weighting function, on electron-irradiated Fe-contaminated and reference samples before and after annealing at 150, 200, and 250 °C for 30 min. Three distinctive peaks, H(0.25), H(0.29), and H(0.34), are only found in the Fe-contaminated samples. These spectra are extracted from rate-window of  $(640 \text{ ms})^{-1}$ .

formation of this layer is not found to cause any electrically defects by itself, as evidenced by the as-irradiated spectrum in Fig. 1(a) showing only the two Fe-related levels in addition to those observed in the reference sample. In fact, pn-junctions formed by the same process, but without intentional Fe-contamination and irradiation, are observed to contain no detectable amount of electrically active defects (not shown). In this respect, the reference sample with the Schottky diode serves also as a reference for the p-n formation process, and not for the Fe contamination only. However, the  $n^+$ -layer may get migrating Fe-species in the near surface region<sup>3</sup> and thus enhance the out-diffusion of Fe from the region probed by the DLTS measurements.

Figure 2 summarises the concentration of the observed defect levels after subsequent annealings (30 min). The data for  $\text{C}_i\text{O}_i$  have been subtracted with  $2 \times 10^{12}$  and  $5 \times 10^{12} \text{ cm}^{-3}$  for the Fe-contaminated and the reference samples, respectively, to increase the clarity of the figure. In the reference samples, the concentration of  $\text{C}_i\text{O}_i$  is stable above 250 °C, in accordance with the dissociation energy of  $\sim 2.0 \text{ eV}$  of the complex.<sup>15</sup> For the  $\text{V}_2$ , a slight decrease takes place after 250 °C, which can be associated with the formation of  $\text{V}_2\text{O}$ ;<sup>16</sup> indeed, a peak appears at 116 K in Fig. 1, with a position of  $E_V + 0.22 \text{ eV}$  and an apparent capture cross-section of  $1 \times 10^{-15} \text{ cm}^2$ , in accordance with previous observations of  $\text{V}_2\text{O}$ .<sup>16,17</sup> For the Fe-contaminated samples, however, a different trend occurs for  $\text{V}_2$  and  $\text{C}_i\text{O}_i$ . Both defects exhibit a reduction in concentration already after 150 °C, with the exception of a sudden increase of  $\text{C}_i\text{O}_i$  at 225 °C. Hence, a different and more complex annealing behavior of the irradiation-induced

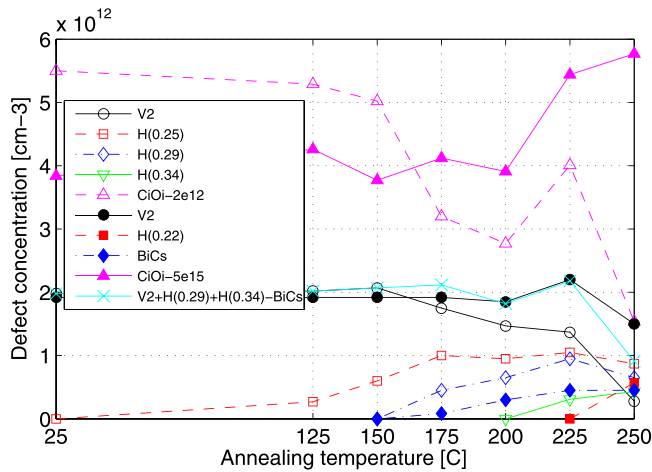


FIG. 2. Evolution of the defect concentrations in Fe-contaminated (open symbol) and reference samples (filled symbol) to subsequent annealings of 30 min. Data from as-irradiated samples are plotted at annealing temperature of 25 °C. “V<sub>2</sub> + H(0.29) + H(0.34) – BiCs” is a result from adding the concentration of V<sub>2</sub>, H(0.29), and H(0.34) in the Fe-contaminated samples and subtracting B<sub>i</sub>C<sub>s</sub> from the reference samples.

defects is unveiled due to the presence of Fe, as will be discussed in more detail later.

Three distinctive peaks are exclusively observed in the Fe-contaminated samples at 130, 136, and 153 K with the corresponding labels of H(0.25), H(0.29), and H(0.34). The Arrhenius plots of these levels are shown in Fig. 3, and the extracted energy level positions are 0.25, 0.29, and 0.34 eV above  $E_V$  with apparent capture cross-sections of  $1 \times 10^{-14}$ ,  $9 \times 10^{-15}$ , and  $2 \times 10^{-14}$  cm<sup>2</sup>, respectively. The data points for H(0.25) and H(0.29) are extracted after simulating the DLTS spectra, as displayed in Fig. 4 (only two rate windows are displayed for clarity).

Figure 3 contains two additional sets of data; one set is extracted from the peak at 135 K in the reference samples after annealing above 150 °C. The Arrhenius plot for the reference sample reveals an energy level position and an appa-

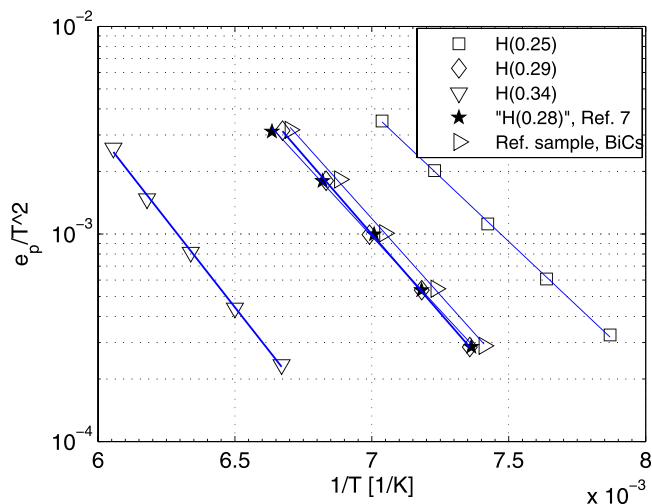


FIG. 3. Arrhenius plot of the three distinctive deep levels in Fe-contaminated samples and two additional sets of data for comparison. The data points for H(0.29) are extracted from the simulated DLTS spectra, partially shown in Fig. 4, and compared with those of B<sub>i</sub>C<sub>s</sub> in the reference samples and from Ref. 7.

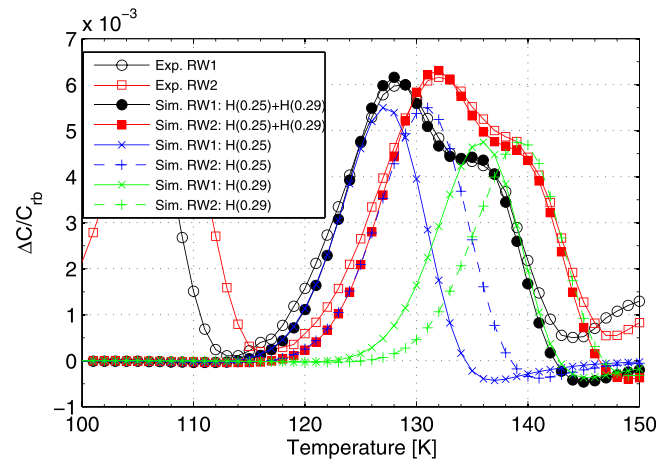


FIG. 4. Experimental (Exp.) and simulated (Sim.) DLTS spectra for the H(0.25) and H(0.29) peaks between 120 to 150 K for rate window 1 (RW1) of (640 ms)<sup>−1</sup> and rate window 2 (RW2) of (320 ms)<sup>−1</sup>.

rent capture cross-section of  $E_V + 0.29$  eV and  $2 \times 10^{-14}$  cm<sup>2</sup>, respectively, and the level is identified as the interstitial boron-substitutional carbon (B<sub>i</sub>C<sub>s</sub>).<sup>18</sup> Based on the similar properties of B<sub>i</sub>C<sub>s</sub> and H(0.29), it may be tempting to attribute H(0.29) solely as B<sub>i</sub>C<sub>s</sub>. However, in addition to the larger concentration in the Fe-contaminated samples than in the reference samples (Fig. 2), the concentration versus depth profiles differ significantly, as shown in Fig. 5. B<sub>i</sub>C<sub>s</sub> remains close to constant as a function of depth in the reference sample, as expected for MeV electron-irradiated samples, while H(0.29) exhibits a substantial increase in concentration towards the bulk. This implies that H(0.29) is not primarily due to B<sub>i</sub>C<sub>s</sub>, but forms when an impurity diffuses from the bulk towards the front surface (n<sup>+</sup>-layer), which act as a sink and depletes the impurity from the bulk. Since Fe is highly mobile at elevated temperatures, it is one main candidate to be involved in H(0.29). The second set added in Fig. 3 is taken from Ref. 7 and is the data for the tentatively assigned divacancy-Fe complex, H(0.28). A close agreement is found between the H(0.29) and H(0.28) data sets.

First, if H(0.29) is assumed to be the donor state of FeV<sub>2</sub>, as predicted in Ref. 6, a second signal at  $E_V + 0.36$  eV with similar amplitude is expected in the DLTS-measurement. However, a peak with the suggested energy level position has a strong overlap with the dominating C<sub>i</sub>O<sub>i</sub> and cannot be readily resolved. Second, Fe and V<sub>2</sub> can be further stabilized from FeV<sub>2</sub> by changing its configuration to VFeV, according to Ref. 6. The predicted energy level position of the single acceptor of VFeV is close to H(0.34) in the present work. H(0.34) is formed after annealing at 225 °C and increases further at 250 °C which indicates a rather stable defect, consistent with the prediction in Ref. 6.

If H(0.34) and H(0.29) are due to Fe-related complexes invoking V<sub>2</sub>, a correlation in the defect concentration versus annealing temperature is a necessary condition. Assuming that B<sub>i</sub>C<sub>s</sub> in the Fe-contaminated samples has the same concentration as in the reference samples, the sum of V<sub>2</sub>, H(0.29), and H(0.34) (Fe-contaminated samples) minus B<sub>i</sub>C<sub>s</sub> (reference samples) is depicted in Fig. 2 (labelled as “V<sub>2</sub> + H(0.29)

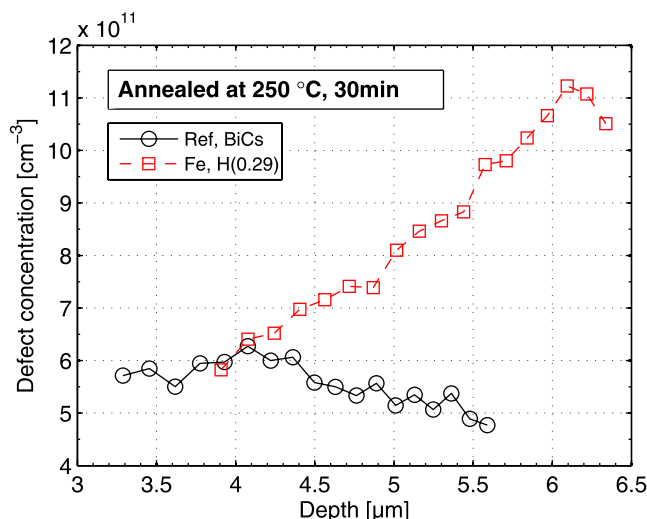


FIG. 5. Concentration versus depth profiles of H(0.29) in the Fe-contaminated samples and the BiCs in the reference samples.

+ H(0.34) – BiCs”). This curve follows closely the concentration of  $V_2$  in the reference samples below 250 °C. Above 250 °C, other reactions start to dominate the annealing of  $V_2$ , like formation of  $V_2O$ .<sup>16,17</sup> From these considerations, there are strong indications that H(0.29) and H(0.34) are caused by complexes formed through reactions between mobile Fe and  $V_2$ , supporting the theoretical predictions in Ref. 6.

H(0.25) appears at 125 °C and remains essentially stable at temperatures above 175 °C (Fig. 2). Although its concentration correlates with the loss of  $C_iO_i$  below 175 °C, suggesting a relation to  $C_iO_i$ , the pattern is not unambiguous above 175 °C. One may speculate that a further (higher order) reaction between Fe and  $C_iO_i$  passivates the H(0.25) complex which will account for the decrease in the concentration of  $C_iO_i$  and possibly also the saturation of H(0.25). However, the literature on interaction between Fe and  $C_iO_i$  is scarce and further investigations should be pursued; for instance with isothermal annealing including reverse biasing.

#### IV. CONCLUSION

Boron-doped and Fe-contaminated Fz silicon samples have been electron-irradiated and investigated for Fe-related

defects using DLTS after isochronal annealing up to 250 °C. Three distinct deep levels are exclusively revealed in the Fe-contaminated samples after annealing. The concentration of two of these ones, H(0.29) and H(0.34), accompany the loss in concentration of  $V_2$ , suggesting an interaction between mobile Fe and  $V_2$ , in accordance with previous theoretical predictions in the literature.

#### ACKNOWLEDGMENTS

This work was funded by the Norwegian Research Council through the project “Hydrogen in solar-grade p-type Si (HydSil)” within the RENERGI program.

- <sup>1</sup>A. A. Istratov, H. Hielsmair, and E. R. Weber, *Appl. Phys. A* **70**, 489 (2000), and references therein.
- <sup>2</sup>J. H. Reiss, R. R. King, and K. W. Mitchell, *Appl. Phys. Lett.* **68**, 3302 (1996).
- <sup>3</sup>M. Syre, S. Karazhanov, B. R. Olaisen, A. Holt, and B. G. Svensson, *J. Appl. Phys.* **110**, 024912 (2011).
- <sup>4</sup>Z.-P. You, M. Gong, J.-Y. Chen, and J. W. Corbett, *J. Appl. Phys.* **63**, 324 (1987).
- <sup>5</sup>B. A. Komarov, *Semiconductors* **38**, 1041 (2004).
- <sup>6</sup>S. K. Estreicher, M. Sanati, and N. G. Szewacki, *Phys. Rev. B* **77**, 125214 (2008).
- <sup>7</sup>C. K. Tang, L. Vines, B. G. Svensson, and E. V. Monakhov, *Phys. Status Solidi C* **9**(10-11), 1992 (2012).
- <sup>8</sup>C. K. Tang, L. Vines, B. G. Svensson, and E. V. Monakhov, *Appl. Phys. Lett.* **99**, 052106 (2011).
- <sup>9</sup>A. A. Istratov, *J. Appl. Phys.* **82**, 2965 (1997).
- <sup>10</sup>B. G. Svensson, A. Hallén, J. H. Svensson, and J. W. Corbett, *Phys. Rev. B* **43**, 2292 (1991).
- <sup>11</sup>H. Malmbeek, L. Vines, E. V. Monakhov, and B. G. Svensson, *Solid State Phenom.* **178–179**, 192 (2011).
- <sup>12</sup>P. M. Mooney, L. J. Cheng, M. Süli, J. D. Gerson, and J. W. Corbett, *Phys. Rev. B* **15**, 3836 (1977).
- <sup>13</sup>J. Lalita, N. Keskitalo, A. Hallén, C. Jagadish, and B. G. Svensson, *Nucl. Instrum. Methods Phys. Res. B* **120**, 27 (1996).
- <sup>14</sup>A. A. Istratov, H. Hielsmair, and E. R. Weber, *Appl. Phys. A* **69**, 13 (1999), and references therein.
- <sup>15</sup>B. G. Svensson and J. L. Lindström, *Phys. Status Solidi A* **95**, 537 (1986).
- <sup>16</sup>M. Mikelsen, E. V. Monakhov, G. Alfieri, B. S. Avset, J. Härkönen, and B. G. Svensson, *J. Phys. Condens. Matter* **17**, S2247 (2005).
- <sup>17</sup>M.-A. Trauwaert, J. Vanhellefont, H. E. Maes, A.-M. V. Bavel, G. Langouche, and P. Clauws, *Appl. Phys. Lett.* **66**, 3056 (1995).
- <sup>18</sup>O. J. Drevinsky, C. E. Cafer, S. P. Tobin, J. C. Mikkelsen, Jr., and L. C. Kimerling, in *MRS Proceedings* (1987), Vol. 104, p. 167.